Direct reaction measurements with a ^{132}Sn radioactive ion beam

K. L. Jones,[1,2] F. M. Nunes,[3] A. S. Adekola,[4,*] D. W. Bardayan,[5] J. C. Blackmon,[5,†] K. Y. Chae,[1,5] K. A. Chipps,[6]
J. A. Cizewski,[2] L. Erikson,[6,§] C. Harlin,[7] R. Hatarik,[2,‖] R. Kapler,[1] R. L. Kozub,[8] J. F. Liang,[5] R. Livesay,[6,‡]
Z. Ma,[1] B. Moazen,[1] C. D Nesaraja,[5] S. D. Pain,[2,5] N. P. Patterson,[7] D. Shapira,[5] J. F. Shriner Jr.,[8] M. S. Smith,[5]
T. P. Swan,[2,7] and J. S. Thomas[7,¶]

[1]*Department of Physics and Astronomy, University of Tennessee, Knoxville, Tennessee 37996, USA*
[2]*Department of Physics and Astronomy, Rutgers University, New Brunswick, New Jersey 08903, USA*
[3]*National Superconducting Cyclotron Laboratory and Department of Physics and Astronomy,*
Michigan State University, East Lansing, Michigan 48824, USA
[4]*Department of Physics and Astronomy, Ohio University, Athens, Ohio 45701, USA*
[5]*Physics Division, Oak Ridge National Laboratory, Oak Ridge, Tennessee 37831, USA*
[6]*Physics Department, Colorado School of Mines, Golden, Colorado 80401, USA*
[7]*Department of Physics, University of Surrey, Guildford, Surrey GU2 7XH, United Kingdom*
[8]*Department of Physics, Tennessee Technological University, Cookeville, Tennessee 38505, USA*

The (d,p) neutron transfer and (d,d) elastic scattering reactions were measured in inverse kinematics using a radioactive ion beam of ^{132}Sn at 630 MeV. The elastic scattering data were taken in a region where Rutherford scattering dominated the reaction, and nuclear effects account for less than 8% of the elastic scattering cross section. The magnitude of the nuclear effects, in the angular range studied, was found to be independent of the optical potential used, allowing the transfer data to be normalized in a reliable manner. The neutron-transfer reaction populated a previously unmeasured state at 1363 keV, which is most likely the single-particle $3p_{1/2}$ state expected above the $N = 82$ shell closure. The data were analyzed using finite-range adiabatic-wave calculations and the results compared with the previous analysis using the distorted-wave Born approximation. Angular distributions for the ground and first-excited states are consistent with the previous tentative spin and parity assignments. Spectroscopic factors extracted from the differential cross sections are similar to those found for the one-neutron states beyond the benchmark doubly magic nucleus ^{208}Pb.

I. INTRODUCTION

A subject of great interest in nuclear structure physics is the evolution of a single-particle structure far from stability and how this can reflect changes in shell structure. Transfer reactions are a powerful probe for investigating the single-particle structure of nuclei [1,2]. Using solid targets with a high stoichiometry of protons or deuterons, for example, it is possible to perform transfer reactions in inverse kinematics on beams of nuclei that cannot easily be made into targets [3]. With the availability of beams of short-lived ions at energies relevant to these studies, that is, of a few mega–electron volts to a few tens of mega–electron volts per nucleon, it is now

possible to conduct transfer reactions with exotic nuclei in inverse kinematics (e.g., Refs. [4–8]). In particular, the single-neutron stripping reaction (d,p) can be performed using beams of fission fragments impinging on targets of deuterated plastic [6,7]. The experiments described here represent the first direct reaction measurements using a beam of short-lived, $t_{1/2} = 40$ s, ^{132}Sn at energies close to the Coulomb barrier.

As transfer reactions selectively populate single-particle or single-hole states, they have particular relevance close to shell closures. With $Z = 50$ and $N = 82$, ^{132}Sn belongs to the select group of nuclei with standard magic numbers of both protons and neutrons. This is seen, for example, through the high energy of the first 2^+ state in the tin isotopes (around 1.2 MeV), compared to the neighboring elements (typically around 500 keV). Additionally, the large discontinuities seen in neutron-rich tin isotopes in both the first 2^+ energy, rising to 4.04 MeV in ^{132}Sn, and the two-neutron separation energy, S_{2n}, falling from 12.56 MeV for ^{132}Sn to 6.38 MeV for ^{134}Sn ($N = 84$), are indicative of the doubly magic nature of ^{132}Sn.

The characterization of the states in ^{133}Sn is critical to understanding the evolution of single-particle structure in this important region of the nuclear chart and to extrapolating the properties of nuclei outside the current reach of detailed experimental study, including those on the astrophysical r-process path. With a low ground state Q value of 0.147 MeV, the ^{132}Sn(d,p) reaction at energies around the
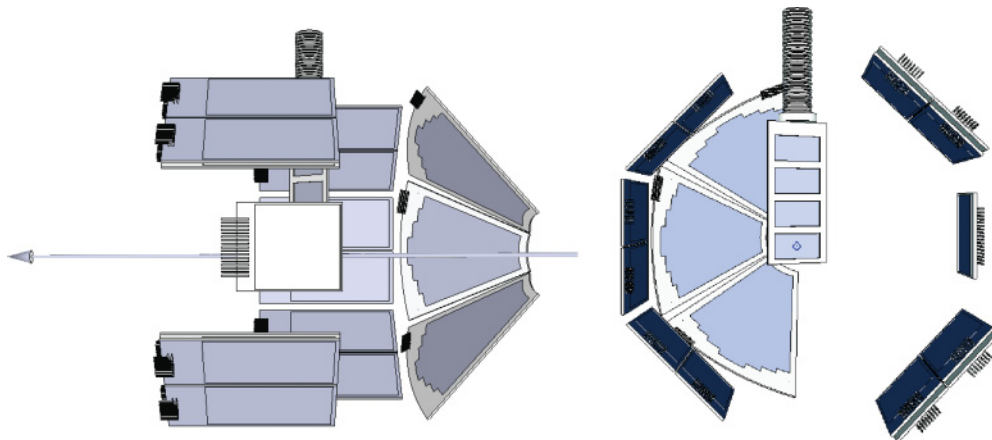
FIG. 1. (Color online) Diagrams from the side (left) and beam (right) views of the experimental setup (not to scale) [9].

Coulomb barrier favorably populates low-energy, low-angular-momentum, single-particle states. The lowest-energy neutron-particle states expected above the $N = 82$ shell closure are $2f_{7/2}$, $3p_{3/2}$, $3p_{1/2}$, $1h_{9/2}$, $2f_{5/2}$, and $1i_{13/2}$. Previous to the current experiment, candidates for all but the $3p_{1/2}$ and the $li_{13/2}$ states had been identified in ^{133}Sn [10,11].

Previous studies of ^{133}Sn have used β decay [10] or the prompt γ decay of fission fragments from ^{248}Cm [11]. The β decay of ^{133}In is dominated by the $(\pi g_{9/2})^{-1}$ configuration, which favors the population of states with spin 7/2, 9/2, or 11/2. Similarly, low-spin states are disfavored in the β-delayed neutron decay of ^{134}In; typically, states within 1 unit of angular momentum to those observed from the β decay are populated. Because the fission process favors fragments with significant angular momentum, the prompt γ rays observed are associated with decay of higher spin excitations on or near the yrast line. Hence, previous studies of ^{133}Sn most likely missed low-spin states.

The information that can be gained from transfer-reaction experiments includes energies and angular distributions of the light-ion ejectiles. The energies provide the excitation energies of the heavy recoil, and the angular distributions can be used to extract the ℓ value of the transfered nucleon. By comparison of the differential cross sections for individual states with those calculated using a reaction model, spectroscopic factors can be extracted. In the region that is well described by Rutherford scattering, elastically scattered target components can be used to accurately normalize the data from transfer. Additionally, the elastic scattering of beams of exotic nuclei could be used to improve optical model potentials away from stability.

Some of the results of the ^{132}Sn(d,p) reaction study have been reported previously [12]. The present paper provides a more detailed presentation of the experimental results, including elastic scattering of deuterons, as well as an interpretation of the data within the ADiabatic Wave Approximation (ADWA).

II. EXPERIMENTAL SETUP

The experiment was performed at the Holifield Radioactive Ion Beam Facility [13] at Oak Ridge National Laboratory. The ^{132}Sn ions were produced from the fission of ^{nat}U

following the bombardment of protons (up to a maximum energy of 50 MeV) using the isotope separation online (ISOL) technique. The beam was purified by extracting tin sulfide molecules and selecting mass $= 164$ at the first-stage separator. Following charge exchange and subsequent breakup of the SnS molecules, ^{132}Sn ions were accelerated to a total energy of 630 MeV in the 25-MV tandem accelerator. The essentially pure ($>90\%$) ^{132}Sn beam impinged on a deuterated polyethylene target with an areal density of 80 μg/cm^2. The target was turned 30° to the beam axis, resulting in an effective target thickness of 160 μg/cm^2, to allow the measurement of emitted particles close to $\theta_{lab} = 90°$.

Scattered light ions and protons emitted from the (d,p) reaction were measured in a system of silicon detectors incorporating the Silicon Detector Array (SIDAR) [14] and an early implementation of the Oak Ridge Rutgers University Barrel Array (ORRUBA) [15], as shown in Fig. 1. SIDAR, placed at backward angles in the laboratory frame for a subsequent experiment, was exposed to a small number of reaction protons, as only the population of $\ell = 0$ states would result in significant numbers of protons at these backward laboratory angles owing to the inverse kinematics of the experiment. The ORRUBA detectors covered polar angles between 69° and 107°. At angles forward of $\theta_{lab} = 90°$, where the detectors were exposed to elastically scattered protons, deuterons, and ^{12}C target constituents, four telescopes of ORRUBA detectors were employed. Three of the telescopes used 140-μm ΔE (energy loss) detectors, and the other used a 65-μm ΔE detector. The second layer of the telescopes and single-layer detectors backward of the elastic scattering region were 1000 μm thick. The high capacitance of both types of ΔE detectors, combined with the necessary resistive layer for charge division, resulted in low signal-to-noise ratios and incomplete charge collection. Subsequent to this measurement nonresistive 65-μm ΔE detectors have been incorporated into the ORRUBA setup. Owing to the poor resolution of the ΔE detectors, the signals were not used in the analysis of the transfer data. Instead, the energy loss in these detectors was reconstructed from the measured residual energy in the E detectors. This impacted the resulting Q-value resolution, leading to a resolution of $\approx$300 keV. The energies and angles of
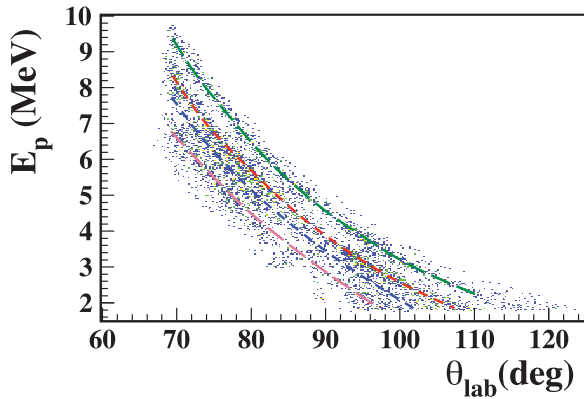
FIG. 2. (Color online) Energy-versus-angle measurements for the protons emitted from the ^{132}Sn(d,p) measurement. Equi-Q-value lines are shown to guide the eye for the ground (green curve), 854-keV (red curve), 1363-keV (blue curve), and 2005-keV (pink curve) states.
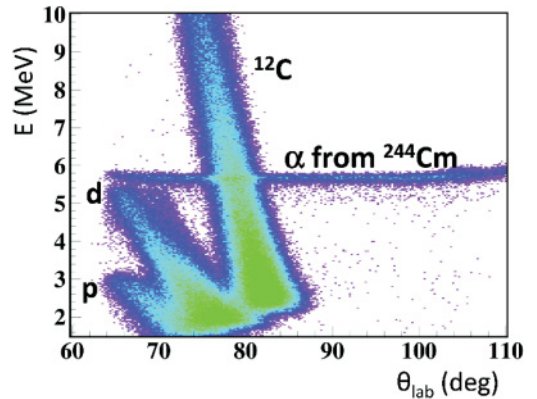

FIG. 3. (Color online) Energy-versus-angle measurements for protons, deuterons, and ^{12}C atoms scattered out of the deuterated polyethylene target, measured in a single ΔE detector. The horizontal line corresponds to the α decay of ^{244}Cm present in the target chamber.

protons emitted from the (d,p) reaction follow well-defined loci dependent on the Q value of the reaction, as shown in Fig. 2. Lines representing the calculated kinematic loci for reactions resulting in ^{133}Sn being produced in its ground and 854-, 1363-, and 2005-keV states are shown to help guide the eye.

III. ELASTIC SCATTERING OF ^{132}Sn ON A DEUTERON TARGET

The purpose of measuring the elastic scattering of the ^{132}Sn beam on a deuteron target was twofold. First, and most importantly, these data can provide a robust method of normalization of the transfer cross sections. Second, in general, elastic scattering data can also be used to constrain the parameters of the optical potential.

In order to establish an absolute cross-section scale for the nucleon-transfer data, the transfer yields have been compared to deuteron elastic scattering yields. The elastic scattering yields were measured in an angular range where the calculated absolute differential cross sections for elastic scattering are dominated by Coulomb effects and are insensitive to the choice of optical model potential.

The elastically scattered deuterons were measured in the 140-μm-thick ΔE detector with the best performance. The most forward center-of-mass angles correspond to the lowest energy elastically scattered particles. Therefore, the angle and energy resolutions degrade appreciably at center-of-mass angles much below $\theta_{c.m.} = 30°$ ($\theta_{lab} = 75°$), as shown in Fig. 3. Data from the ^{132}Sn(d,d) reaction were extracted for $28.4° \leqslant \theta_{c.m.} \leqslant 39.3°(70.4° \leqslant \theta_{lab} \leqslant 75.8°)$ (Fig. 4). Over this range of angles, the excursions from pure Rutherford scattering were less than 8%. In order to be able to use the elastic scattering data to normalize the transfer cross sections, the contribution coming from nuclear scattering had to be taken into account.

In Fig. 4, in comparison with the data, the calculated angular distributions using two optical potentials based on the ^{124}Sn deuteron optical potential of Strömich *et al.* [16] are displayed. Set S1 includes a surface imaginary term and S2 includes a

volume imaginary term. Considering a 5% uncertainty in the normalization of the data, fits for both cases result in a $\chi^2 \approx 1$. While both S1 and S2 may seem like adequate choices for the range where data are available, they differ significantly over a wider angular range, and it is not clear that either would be adequate to describe elastic scattering of deuterons off ^{132}Sn (note that the potentials from [16] were obtained from data on stable isotopes including backward angles). Subsequently, a series of fits of the optical potential parameters was performed. Shown in Fig. 4 are the results of two such fits (fit 1 based on S1 and fit 2 based on S2). Not surprisingly, the fits demonstrated that the optical potential parameters are not well constrained by this narrow angular range. Nevertheless, the resulting elastic scattering cross sections in this range do not change by more than 5% owing to the dominance of the Coulomb potential. Set S2 was used to normalize the (d,p) data. A systematic uncertainty of 5% coming from this normalization was applied to the cross sections from the transfer data.

IV. THE ^{132}Sn(d,p) REACTION IN INVERSE KINEMATICS

The Q value for the population of ^{133}Sn via the (d,p) reaction was calculated on an event-by-event basis from the measured angle and energy of the emitted proton. The energy of the beam was corrected for energy loss in the target, assuming that the reaction occurred in the center of the target, as was the energy of the proton. Three low-lying, low-spin states had been previously observed in ^{133}Sn—the ground state, the 854-keV, and the 2005-keV excited states—with tentative spin assignments of $7/2^-$, $3/2^-$, and $5/2^-$, respectively. Four peaks were observed in the Q-value spectrum (Fig. 5) corresponding to these states, as well as a newly observed state. The excitation energy of this new state, interpolated from the Q values of the other three peaks, was determined to be 1363 ± 31 keV. Figure 6 summarizes the systematics of single-particle states in $N = 83$ isotones, including the new 1363-keV candidate for the $p_{1/2}$ state. The smooth variation of the energy of $1/2^-$ states in $N = 83$ isotones, including the candidate in ^{133}Sn,
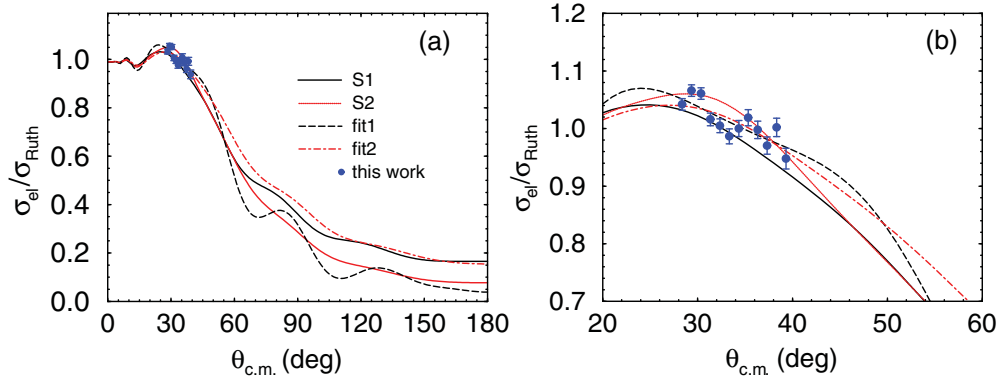
FIG. 4. (Color online) (a) Ratio of measured-to-Rutherford cross sections for the ^{132}Sn(d,d) reaction. Solid curves are calculations using potentials of Strömich *et al.* [16], one with a surface imaginary term [S1; solid (black) curve] and the other with a volume imaginary term [S2; dotted (red) curve]. Examples of the result of χ^2 fitting to S1 and S2 are shown as fit 1 [dashed (black) curve] and fit 2 [dot-dashed (red) curve], respectively. (b) An expanded view of the region covered by the data.

supports this assignment; however, more evidence is required before the assignment can be considered firm.

To confirm single-particle assignments for the ground and first-excited states, angular distributions of protons emitted following the (d,p) reaction were measured (see Fig. 7) and compared to calculations assuming either an $\ell = 1$ or an $\ell = 3$ transfer (these calculations are described in Sec. V). It should be noted that only *p*-wave or *f*-wave states are expected to be significantly populated using a low-energy (d,p) reaction in $N = 83$ nuclei near ^{132}Sn. For example, if the $9/2^-$ state were populated at 1561 keV, a resulting angular distribution peaking at less than 1 mb/sr could be expected for a spectroscopic factor of unity; hence the differential cross section is at least an order of magnitude lower than that for the observed states.

The angular distributions were extracted from the data by fitting four Gaussians to the four states shown in Fig. 5 at each angle. Figure 7(a) shows the measured angular distribution of protons following population of the ground state, in the center of mass, and calculations assuming transfer to the $2f_{7/2}$ and $3p_{3/2}$ states. Both calculations agree with the ground-state
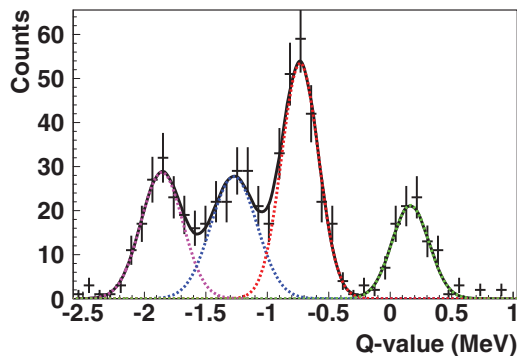
data across most of the range of angles; however, the $\ell = 3$ calculation is preferred at the most forward angles (around $\theta_{c.m.} = 20°$). For the 854-keV state [Fig. 7(b)] an $\ell = 1$ transfer reproduces the data, particularly at more forward angles. The assignments of the $2f_{7/2}$ and $3p_{3/2}$ states are therefore confirmed.

The population of the higher excited levels in ^{133}Sn led to lower energy protons being detected in the ORRUBA detectors. As these detectors use charge division to extract position information, it was necessary to receive a significant signal from both ends of the detector in order to measure the energy and position of the charged particle. This became increasingly difficult at lower proton energies. Additionally, if the proton strikes near one end of the strip, the signal at the far end is degraded in quality. In particular, it is spread out in time, which can lead to incomplete charge collection or, in the worst cases, the signal not arriving within the time required by the acquisition gate. For these reasons, only the central portion of the ORRUBA detectors was able to provide data for the low-energy protons emitted from the population of the 1363- and 2005-keV states. Hence angle-integrated cross sections, rather than angular distributions, are shown in Fig. 8.
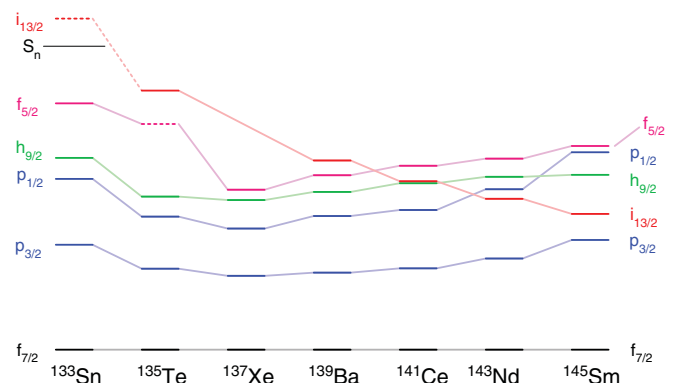

FIG. 5. (Color online) Q-value spectrum for the ^{132}Sn(d,p)^{133}Sn reaction with a 630-MeV ^{132}Sn beam. The solid (black) line shows a fit including four peaks: the ground state (green curve), the 854-keV state (red curve), the previously unobserved 1363-keV state (blue curve), and the 2005-keV state (magenta curve).

FIG. 6. (Color online) Single-particle states in the $N = 83$ even-Z isotones between ^{145}Sm and ^{133}Sn. Data taken from the Evaluated Nuclear Structure Data File [17], Ref. [18], and present results.
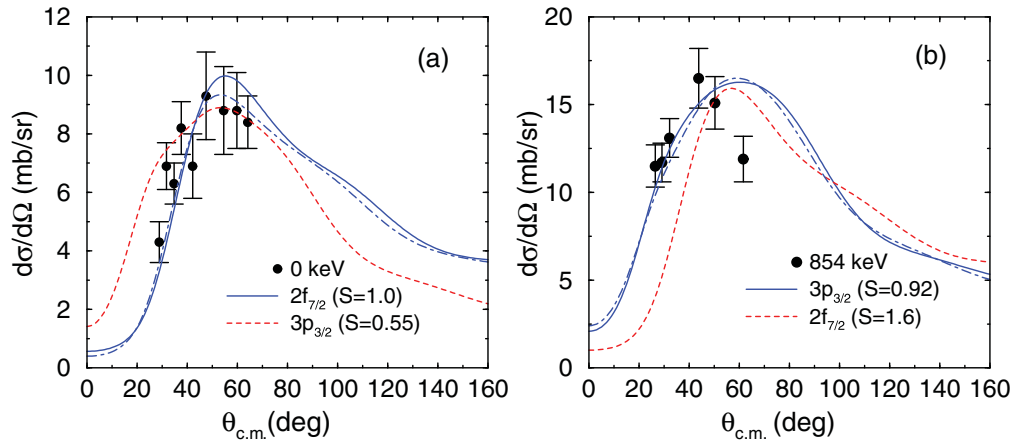
FIG. 7. (Color online) Angular distributions of protons in the center of mass from the ^{132}Sn(d,p)^{133}Sn reaction for the ground (a) and 854-keV (b) states. Calculations assuming the nlj assignments in Table I, using ADWA-CH, are shown by the solid (blue) curve. Similar calculations assuming the nearest expected alternate f-wave or p-wave single-neutron state are shown by the dashed (red) curve. Numbers in parentheses give the spectroscopic factors used to fit the calculation to the data. Calculations using ADWA-BG assuming the $n\ell j$ assignments in Table I are shown by the dot-dashed (blue) curve.

The 2005-keV state had been previously observed in β decay and assigned $(5/2^-)$, consistent with a population from a high-spin parent. If indeed this is the expected $2f_{5/2}$ level, the spectroscopic factor is consistent with 1. An alternative $3p_{1/2}$ assignment is inconsistent with its observation in β decay. On the other hand, the 1363-keV state had not been previously observed via β decay, β-delayed neutron decay [10], or γ decay following fission [11]. Therefore, it is likely that this is a lower spin state and a good candidate for the expected $3p_{1/2}$ state. The assignments of the 1363-keV state as $3p_{1/2}$ and the 2005-keV state as $2f_{5/2}$ are also supported by the systematics summarized in Fig. 6. The extraction of spectroscopic factors was made by fitting the reaction calculation curves to the data in the region of the first peak, that is, in the range $20° < \theta_{c.m.} < 70°$, for the ground and first-excited states. The fit for the 854-keV state is most sensitive to the forward-angle points, with the most backward-angle point having a marginal effect on the fit. The uncertainty in this fitting procedure is quantified in Table VII.

V. REACTION ANALYSIS

The initial analysis [12] of the ^{132}Sn(d,p) reaction was performed in the finite-range (FR) distorted-wave Born approximation (DWBA) framework, with the code FRESCO [19]. The optical model parameters were taken from Strömich *et al.* [16]. For completeness, these results for the spectroscopic factors and asymptotic normalization coefficients [20] are summarized in Tables I and II, respectively. The same framework was also used to analyze the ^{208}Pb(d,p) reaction. Those results, and results from choosing global optical model parameters, were also reported in Ref. [12] and the associated Supplemental Material.

Although traditionally the one-step DWBA has been widely used to analyze (d,p) reactions, it has long been known that it is often inaccurate. Johnson and Soper [21] showed the importance of including deuteron breakup explicitly and devised a practical method for analyzing (d,p) reactions that is nonperturbative, the so-called ADWA. Its simplicity arises partly from the use of the zero-range approximation for the deuteron. An FR version of this method [22] has recently been applied to a wide range of (d,p) reactions [23], showing the importance of performing a full FR calculation. This method, referred to as the FR-ADWA, is the method used here to analyze all of the transfer data. Within this method, the deuteron adiabatic wave is constructed from nucleon optical potentials, considerably reducing the optical parameter uncertainties.

TABLE I. Spectroscopic factors S of the four single-particle states populated by the ^{132}Sn(d,p)^{132}Sn reaction extracted using the DWBA [12] and ADWA formalisms. Error margins listed include only experimental uncertainties. Values extracted from the ADWA-CH are considered the most reliable and are listed in boldface.

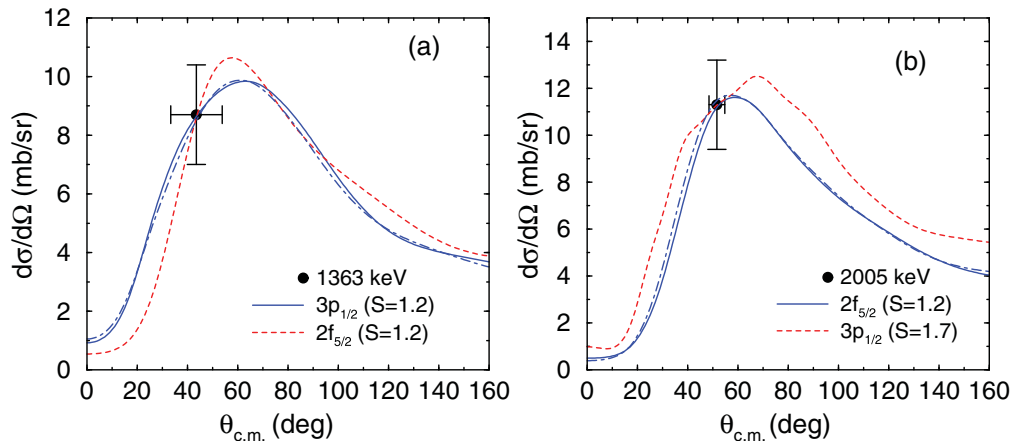| E_x (keV)	nlj	Spectroscopic factor		
		DWBA	FR-ADWA-BG	**FR-ADWA-CH**
0	$2f_{7/2}$	0.86 ± 0.07	1.2 ± 0.1	**1.00 ± 0.08**
854	$3p_{3/2}$	0.92 ± 0.07	1.0 ± 0.1	**0.92 ± 0.07**
1363 ± 31	$(3p_{1/2})$	1.1 ± 0.2	1.2 ± 0.3	**1.2 ± 0.2**
2005	$(2f_{5/2})$	1.1 ± 0.2	1.3 ± 0.3	**1.2 ± 0.3**

FIG. 8. (Color online) Integrated cross section measurements from the ^{132}Sn(d,p)^{133}Sn reaction for the 1363-keV state (a) and 2005-keV state (b). Differential cross section calculations assuming the assignments in Table I, using ADWA-CH, are shown as the solid (blue) curve. Similar calculations assuming the nearest expected alternate f-wave or p-wave single-neutron state are shown by the dashed (red) curve. Numbers in parentheses give the spectroscopic factors used to fit the calculation to the data. Calculations using ADWA-BG assuming the $n\ell j$ assignments in Table I are shown by the dot-dashed (blue) curve.

Calculations for the ^{132}Sn(d,p)^{133}Sn reaction were performed in postform using the reaction code FRESCO [19]. A realistic Reid interaction [24] was used for the deuteron with the neutron-proton potential, V_{np}, in the transfer operator. The global optical model parameters CH89 [25] were used for all nucleon optical potentials. The deuteron adiabatic potential was generated with TWOFNR [26]. One important source of ambiguity in modeling transfer reactions is the choice of the single-particle parameters used for the overlap function, in this case, ^{133}Sn relative to ^{132}Sn. Even if radii predicted by density functional theory [27] for the tin isotopes were used, the geometry of the valence neutron would still carry large uncertainties. Therefore, the mean field was fixed to a standard Woods-Saxon shape with radius parameter $r = 1.25$ fm and diffuseness parameter $a = 0.65$ fm.

FR-ADWA angular distributions for single-neutron transfer to all measured states are presented in Figs. 7 and 8 using the preferred $n\ell j$ assignment [solid (blue) line], as indicated in Tables I and II, and an alternate $n\ell j$ assignment [dashed (red) line]. These assignments represent the nearest expected $\ell = 1$ and $\ell = 3$ single-particle states. The calculations have been scaled to the data, with the scaling representing the spectroscopic factor, shown in the legends to Figs. 7 and 8 and also summarized in Table I.

The normalization of the many-body overlap function of ^{133}Sn relative to ^{132}Sn for large neutron-^{132}Sn distances is characterized by the asymptotic normalization coefficient (ANC), usually denoted C [20]. The squares of the ANCs, C^2, for the various states are summarized in Table II.

To evaluate the uncertainty in the normalization of the transfer cross section, the dependence on (a) the nucleon optical potential and (b) the ^{132}Sn mean field generating the neutron valence orbitals in ^{133}Sn needs to be understood.[1]

---

[1]Note that at this beam energy, excitation of the ^{132}Sn core is negligible.

Concerning point a, the data were reanalyzed using optical model parameters from Bechetti-Greenlees (BG) [28]. FR-ADWA analysis requires nucleon potentials, whereas the DWBA uses deuteron optical potentials, the latter being far more ambiguous. The results of the FR-ADWA-BG calculations are shown by the thin dot-dashed lines in Figs. 7 and 8 after scaling to the data. The resulting normalization factors are listed in Table I. Apart from minor changes in the shape of the distributions, differences in the spectroscopic factors are 15% for the ground state, 13% for the state at 854 keV, 11% for the state at 1363 keV, and 10% for the state at 2005 keV. Note that neither BG nor CH89 has been developed for neutron-rich nuclei or for reactions at 5 MeV/nucleon. CH89 is a more modern interaction and, in the last few years, has been successfully used to describe reactions with rare isotopes, including reactions at low energies. The comparison between CH89 and BG provides an indication of the uncertainty introduced by the nucleon optical potentials. These could be significantly reduced by determining proton optical potentials on neutron-rich nuclei in this mass region.

Concerning the ^{132}Sn mean field, FR-ADWA calculations were repeated using the radius parameter $r = 1.2$ fm and diffuseness parameter $a = 0.6$ fm. The shapes of the angular distributions do not change when the geometry of the bound

TABLE II. Asymptotic normalization coefficients (ANCs) of the four single-particle states populated by the ^{132}Sn(d,p)^{132}Sn reaction. Listed error margins include only experimental uncertainties.

		C^2 (fm^{-1})	
E_x (keV)	nlj	DWBA	FR-ADWA-CH
0	2f7/2	0.64 ± 0.05	0.82 ± 0.07
854	3p3/2	5.6 ± 0.4	6.5 ± 0.5
1363 ± 31	(3p1/2)	2.6 ± 0.6	2.9 ± 0.6
2005	(2f5/2)	$(0.9 \pm 0.2) \times 10^{-3}$	$(1.2 \pm 0.3) \times 10^{-3}$

TABLE III. Data from the elastic scattering of ^{132}Sn on a deuteron target. The cross section is expressed as a ratio to the calculated Rutherford cross section. Uncertainties listed here are purely statistical. Overall uncertainties are dominated by systematics at a level of 5%.

$\theta_{c.m.}$ (deg)	Ratio to Rutherford cross section
28.4	1.042 ± 0.010
29.4	1.066 ± 0.010
30.4	1.061 ± 0.010
31.4	1.016 ± 0.011
32.4	1.005 ± 0.012
33.4	0.987 ± 0.013
34.3	1.000 ± 0.014
35.3	1.019 ± 0.014
36.3	0.998 ± 0.015
37.3	0.970 ± 0.015
38.3	1.002 ± 0.016
39.3	0.948 ± 0.018

state is varied. While spectroscopic factors increase by up to 40%, the extracted ANCs remain essentially the same, confirming that this reaction is mostly peripheral and therefore not sensitive to details of the wave function in the interior.

Although the FR-ADWA starts from the three-body Hamiltonian n + p + Sn and goes well beyond the DWBA, it does not provide an exact solution to the three-body problem. In order to treat the three-body dynamics fully, a complete Faddeev solution would be necessary. Faddeev methods in momentum space (usually referred to as AGS, for Alt, Grassberger, and Sandhas) have been applied to nucleon-transfer reactions [29] and have been used to determine uncertainties associated with the FR-ADWA [30]. Given the technical difficulties of AGS methods in the treatment of the Coulomb part of the interaction when heavy nuclei are involved, calculations for ^{132}Sn are not available at present.

VI. DISCUSSION

The spectroscopic factors for the four states in ^{133}Sn extracted here, using the FR-ADWA, are all compatible with

TABLE IV. Differential cross sections measured for the ^{132}Sn(d,p)^{133}Sn$_{g.s.}$ reaction.

$\theta_{c.m.}$ (deg)	$d\sigma/d\Omega$ (mb/sr)
28.8	4.3 ± 0.7
31.7	6.9 ± 0.8
34.7	6.3 ± 0.7
37.6	8.2 ± 0.9
42.1	6.9 ± 1.1
47.5	9.3 ± 1.5
54.5	8.8 ± 1.5
59.8	8.8 ± 1.3
64.1	8.4 ± 0.9

TABLE V. Differential cross sections measured for the ^{132}Sn(d,p)^{133}Sn reaction to the 854-keV excited state.

$\theta_{c.m.}$ (deg)	$d\sigma/d\Omega$ (mb/sr)
26.4	11.5 ± 1.2
29.1	11.7 ± 1.1
32.1	13.1 ± 1.1
43.8	16.5 ± 1.7
50.2	15.1 ± 1.5
61.6	11.9 ± 1.3

unity, within experimental and theoretical uncertainties, as summarized in Figs. 7 and 8 and Table I. This was also reported in the previous analysis, although, as pointed out earlier, the DWBA analysis in Ref. [12] has larger uncertainties owing to the ambiguities in the deuteron potential. Because the absolute values of S depend strongly on the choice of the single-particle parameters, ^{208}Pb(d,p)^{209}Pb was also analyzed [12] with a consistent set of parameters. Extracted spectroscopic factors were found also to be close to 1. This serves to further strongly validate that the $N = 82$ shell closure is very robust in this region and ^{132}Sn is a good doubly magic nucleus.

While it is accepted that spectroscopic factors are model dependent, ANCs are largely insensitive to the parametrization of the geometry of the bound state and the optical model parameters. For this reason they are more reliable quantities for use in analyzing peripheral reactions, such as transfer reactions at energies near the Coulomb barrier. Because the ^{132}Sn(d,p) reaction reported here is very peripheral, ANCs can be extracted with virtually no uncertainties coming from the description of the overlap function. Therefore, the experimental uncertainties, as listed in Table II, reflect the total uncertainties in the ANCs. This is the first time that ANCs for states in this region of the nuclear chart have been determined.

Spectroscopic factors are not observables but, rather, are deduced from cross sections. Therefore, it is crucial to understand the values listed in Table I within a larger context. There has been discussion in the literature about extraction of spectroscopic factors from different types of reactions. Spectroscopic factors extracted from (e,e'p) reactions are significantly reduced compared to those from transfer measurements using the standard DWBA, as noted by Kramer *et al*. [31]. Similarly, knockout experiments lead to reduced values of S for all but the most weakly bound nucleons [32]. The apparent disagreement between transfer and knockout is reduced when carefully taking into account all sources of uncertainty in the reaction theory [30].

TABLE VI. Integrated cross sections measured for the ^{132}Sn(d,p)^{133}Sn reaction to the 1363-, and 2005-keV excited states.

E_x (keV)	Range of $\theta_{c.m.}$ (deg)	$d\sigma/d\Omega$ (mb/sr)
1363	33.3–54.0	8.7 ± 1.7
2005	48.4–54.7	11.3 ± 1.9

TABLE VII. Sources of experimental uncertainty in spectroscopic factors and ANCs.

E_x (keV)	Percentage uncertainty			
	Q-value fitting	Normalization	Fitting to angular distribution	Total
0	4.0	5	5	8
854	3.5	5	5	8
1363	6.4	5	20	22
2005	7.0	5	20	22

When the extreme quenching of spectroscopic factors originating from knocking out deeply bound particles was observed [32], one might have assumed that these would correspond to short-range correlations missing from the shell model. More recently, structure models have found it hard to corroborate this assumption. Large-scale shell model calculations with particle-vibrational couplings [33] were able to reproduce the large reductions and thus suggest that the large reduction of strength cannot be interpreted as coming uniquely from short-range correlations. Coupled-cluster calculations for spectroscopic factors for proton removal [34] also show significant quenching of spectroscopic factors when coupling to the continuum is included, again reinforcing that the reduction is caused by more complex mechanisms.

While reductions in S compared to large-scale shell model calculations are generally not observed when using a standard analysis of transfer reactions [35], it is clear that transfer reactions have a strong dependence on the single-particle parameters chosen to describe the many-body overlap function [36]. Lee and collaborators observed that when the geometry of the bound-state potential is constrained using radii from Hartree-Fock calculations, the values of S are reduced and can be made consistent with those from (e,e'p) within error bars [37]. Another aspect that has been considered is the nonlocality in the bound-state interaction, which is known to reduce spectroscopic factors [31]. Alternate forms of determining the overlap function have been proposed [38]. In the current work, a Woods-Saxon potential with standard radius and diffuseness was used for the bound state and no non-locality corrections were introduced.

VII. CONCLUSIONS

The elastic scattering and neutron transfer onto a 630-MeV beam of ^{132}Sn have been studied in inverse kinematics, using a CD$_2$ target. The elastic scattering data were measured at angles where the Rutherford scattering dominated and nuclear effects accounted for less than 8% of the elastic scattering cross section, with different optical models agreeing to within 5%. This allowed for a reliable normalization of the transfer data, but the angular range was too narrow to constrain the deuteron optical potential. Four excited states in ^{133}Sn were populated in the ^{132}Sn(d,p) reaction in inverse kinematics, the ground, 854- and 2005-keV states that had been previously observed, as well as a newly observed state at 1363 keV. The analysis of the angular distributions support $7/2^-$-$2f_{7/2}$ and $3/2^-$-$3p_{3/2}$ assignments to the ground and first-excited

states, respectively. The neutron-transfer data were analyzed within the FR adiabatic wave method. Within this approach, the deuteron wave is determined from nucleon, rather than deuteron, optical potentials and two choices of nucleon optical potentials were used. Both the spectroscopic factors and the asymptotic normalization coefficients were extracted, the latter being independent of the model used to describe the bound state in ^{133}Sn. The spectroscopic factors for all of these states are consistent with $S = 1$ for the proposed assignments. For a standard parameter choice for the mean field of the valence neutron in ^{133}Sn, results are consistent with ^{132}Sn being an excellent closed core.

APPENDIX: DATA

Data are tabulated below for the ^{132}Sn(d,d)^{132}Sn and ^{132}Sn(d,p)^{133}Sn reactions in inverse kinematics. The elastic scattering data shown in Fig. 4 are presented in Table III as a ratio of the measured cross section to that calculated for pure Rutherford scattering. The data from the neutron-transfer reaction, as shown in Figs. 7 and 8, were tabulated in the Supplementary Material of Ref. [12] and are repeated here in Tables IV, V, and VI for completeness.

The uncertainties in the spectroscopic factors and ANCs originating from ambiguities in reaction calculations, in particular, from the choice of optical potential, are not included in Tables I and II. As the relevant measured quantity for extracting spectroscopic factors is the differential, or integrated, cross section, the main sources of experimental uncertainty are

the extraction of population strength from fitting the Q-value spectra (Q-value fitting) and normalization of the data using the elastic scattering data as shown in Fig. 4 and Table III. There is an additional source of uncertainty arising from the fitting of the calculated angular distribution to the data, which

includes the statistical uncertainty in each data point. A breakdown of the contributions to the uncertainties in spectroscopic factors and ANCs is reported in Table VII. These contributions, as well as the total uncertainty, are given as a percentage of S or the ANC.

[1] N. K. Glendenning, in *Nuclear Spectroscopy and Reactions, Part D*, edited by J. Cerny (Academic Press, New York, 1975).

[2] G. Satchler, *Direct Nuclear Reactions* (Oxford University, Oxford, 1983).

[3] G. Kraus *et al.*, Z. Phys. A **340**, 339 (1991).

[4] J. S. Winfield, W. N. Catford, and N. A. Orr, Nucl. Instrum. Methods Phys. Res. Sec. I **396**, 147 (1997).

[5] K. E. Rehm *et al.*, Phys. Rev. Lett. **80**, 676 (1998).

[6] J. S. Thomas *et al.*, Phys. Rev. C **71**, 021302 (2005).

[7] J. S. Thomas *et al.*, Phys. Rev. C **76**, 044302 (2007).

[8] K. Wimmer *et al.*, Phys. Rev. Lett. **105**, 252501 (2010).

[9] K. T. Schmitt (private communication, 2011).

[10] P. Hoff *et al.* (ISOLDE Collaboration), Phys. Rev. Lett. **77**, 1020 (1996).

[11] W. Urban *et al.*, Eur. Phys. J. A **5**, 239 (1999).

[12] K. L. Jones *et al.*, Nature (London) **465**, 454 (2010).

[13] J. R. Beene, D. W. Bardayan, A. G. Uribarri, C. J. Gross, K. L. Jones, J. F. Liang, W. Nazarewicz, D. W. Stracener, B. A. Tatum, and R. L. Varner, J. Phys. G **38**, 024002 (2011).

[14] D. W. Bardayan *et al.*, Phys. Rev. Lett. **83**, 45 (1999).

[15] S. D. Pain *et al.*, Nucl. Instrum. Methods Phys. Res. Sec. B **261**, 1122 (2007).

[16] A. Strömich, B. Steinmetz, R. Bangert, B. Gonsior, M. Roth, and P. von Brentano, Phys. Rev. C **16**, 2193 (1977).

[17] [http://www.nndc.bnl.gov/ensdf/] (2011).

[18] S. D. Pain, private communication (2011).

[19] I. Thompson, Comput. Phys. Rep. **7**, 167 (1988).

[20] D. Y. Pang, F. M. Nunes, and A. M. Mukhamedzhanov, Phys. Rev. C **75**, 024601 (2007).

[21] R. C. Johnson and P. J. R. Soper, Phys. Rev. C **1**, 976 (1970).

[22] R. C. Johnson and P. C. Tandy, Nucl. Phys. A **235**, 56 (1974).

[23] N. B. Nguyen, F. M. Nunes, and R. C. Johnson, Phys. Rev. C **82**, 014611 (2010).

[24] R. V. Reid, Ann. Phys. **50**, 411 (1968).

[25] R. L. Varner, W. J. Thompson, T. L. McAbee, E. J. Ludwig, and T. B. Clegg, Phys. Rep. **201**, 57 (1991).

[26] M. Igarashi and M. Toyama, Computer program TWOFNR, University of Surrey version (2008).

[27] J. Terasaki, J. Engel, M. Bender, J. Dobaczewski, W. Nazarewicz, and M. Stoitsov, Phys. Rev. C **71**, 034310 (2005).

[28] F. D. J. Becchetti and G. W. Greenlees, Phys. Rev **182**, 1190 (1969).

[29] A. Deltuva and A. C. Fonseca, Phys. Rev. C **79**, 014606 (2009).

[30] F. M. Nunes, A. Deltuva, and J. Hong, Phys. Rev. C **83**, 034610 (2011).

[31] G. J. Kramer, H. P. Blok, and A. Lapikás, Nucl. Phys. **679**, 267 (2001).

[32] A. Gade *et al.*, Phys. Rev. C **77**, 044306 (2008).

[33] C. Barbieri, Phys. Rev. Lett. **103**, 202502 (2009).

[34] Ø. Jensen, G. Hagen, M. Hjorth-Jensen, B. Alex Brown, and A. Gade, Phys. Rev. Lett. **107**, 032501 (2011).

[35] J. Lee, M. B. Tsang, and W. G. Lynch, Phys. Rev. C **75**, 064320 (2007).

[36] A. M. Mukhamedzhanov and F. M. Nunes, Phys. Rev. C **72**, 017602 (2005).

[37] J. Lee, J. A. Tostevin, B. A. Brown, F. Delaunay, W. G. Lynch, M. J. Saelim, and M. B. Tsang, Phys. Rev. C **73**, 044608 (2006).

[38] N. K. Timofeyuk, Phys. Rev. Lett. **103**, 242501 (2009).